Arab J. Nucl. Sci. Appl, Vol 52, 3, 43-55(2019)

Arab Journal of Nuclear Sciences and Applications

ISSN 1110-0451 ***Web site: ajnsa.journals.ekb.eg*** **(ESNSA)**

Preparation and Evaluation of ^{177}Lu-TDTMP: A Potential Theranostic Agent for Bone Metastases

O.A. El-Kawy[1*], H.M. Talaat[1] and A. Mohty[2]

[1]*Labelled Compounds Department, Hot Laboratories Center, Atomic Energy Authority, Cairo, Egypt*
[2]*Radioactive Isotopes and Generators Department, Hot Laboratories Center, Atomic Energy Authority, Cairo, Egypt*

Received 17 th Sep 2018
Accepted 24th Apr 2019

^{177}Lu was produced in high-specific activity and excellent radionuclidic purity by thermal neutron bombardment of ^{176}Yb target. Tetramethylene diamine tetramethylenephosphonic acid (TDTMP) was radiolabeled with ^{177}Lu and the complexation parameters were studied and optimized: 8.4 µg TDTMP, ~243 µCi of ^{177}Lu activity, pH= 8 and the reaction mixture was kept at room temperature for 30 min. The complex was formed with high yield (>99%) and retained its stability for more than 14 days. The complex structure was predicted and its binding to target enzyme was assessed. A biodistribution study carried out in normal and tumorized Wister rats showed a significant skeletal uptake, the ^{177}Lu-TDTMP, the results clearly indicated that it has high affinity for bone mineral. Femur and tibia uptakes of the labelled complex were ~ 6.4 % and ~7.1 % at 3 hours post injection compared to ~ 4 % and ~ 4.3 % in case of ^{177}LuCl$_3$. Thereafter, the uptakes increased continuously to a maximum of ~ 7.9 % and ~ 8.3 % at 48 hours after injection were noticed.

Keywords: *Bisphosphonate / Bone metastases / ^{177}Lu / TDTMP / Biodistribution / Theranostics*

Introduction

Metastatic bone lesion (MBL) is a major clinical concern associated with an obvious mortality and morbidity [1]. MBL is commonly observed in advanced state of many cancers especially breast, lung, prostate and bladder carcinoma [2,3]. Its incidence is increasing and can reach 95% depending on the primary cancer type [4]. The special bone microenvironment allows tumor cells, carried by vascular niche, to survive [5]. Adhering to the bone, the tumor cells secret signaling molecules such as parathyroid hormone-related peptide (PTHrP) and interleukin-8/11 (IL-8/11) which recruit osteoclast activity and interrupt the RANKL (receptor activator of nuclear factor κβ ligand) communication between the osteoblasts and osteoclasts. The enhanced osteoclast activity releases growth factors and Ca^{2+} embedded in the bone matrix, which increases tumor cell proliferation [6]. The uncontrolled increased metabolic activity of bone cells benefits the tumor proliferation and supports its growth deeper in the bone tissue, causing disabling bone pain and pathological fractures. At a later stage, the tumor can even invade the marrow causing a bone marrow carcinosis. At the point of painful MBL, palliative therapy to improve the patient quality of life, is a crucial goal to achieve [7-9].

Radiation therapy continues to of a high standard for palliative care of painful MBL [10]. However, the diffuse nature of the disease limits the utilization of the external beam radiation [8]. There is a need for an effective systemic targeted radiotherapy able to deliver high doses to tumor treating multiple metastasis while rendering minimum dose to bone marrow [11]. Bone seeking

Corresponding author: hanan92_harb@yahoo.com
DOI: 10.21608/ajnsa.2019.5151.1118

radiopharmaceuticals are promising agents for MBL diagnosis and therapy [11-13].

Lutetium-177 is an attractive radioisotope for the treatment of skeletal metastasis owing to its considerable nuclear decay characteristics and ready availability [14]. It decays with a half-life of 6.71 days to the stable ground state of ^{177}Hf by emission of low energy β^- particles [Emax of 497 KeV (78.6%), 384 KeV (9.1 %) and 176 KeV (12.2 %)] with mean penetration range of 670 µm [15]. Hence, it produces minimum bone marrow suppression while simultaneously delivering the appropriate dose upon accumulation in skeletal lesions offering a distinct advantage over ^{89}Sr and ^{32}P [5]. ^{177}Lu also emits adequate energy ɣ-photons [113 KeV (6.4 %) and 208 KeV (11%)] in low abundance which is ideally suited for carrying out scintigraphic studies and dosimetric evaluation, thereby enabling diagnosis and monitoring *in vivo* localization in addition to therapeutic effect [1, 4]. The optimal half-life of ^{177}Lu is longer than ^{153}Sm and ^{186}Re providing logistic advantages for facilitating supply to places far away from the reactors and providing the required time period for separation chemical processing, radiopharmaceuticals production and quality control and administration to patient [16]. It is also much shorter than ^{89}Sr and ^{32}P hence offers a faster rate dose delivery for therapeutic purposes [5].

Several phosphonate ligands chelated to different β emitting radionuclides have been investigated for their bone uptake characteristics [1, 4]. However, ethylene diamine tetramethylenephosphonate (EDTMP) continues to be the most widely used ligand and ^{153}Sm-EDTMP is now a well-accepted radiopharmaceutical for pain palliation in skeletal metastases [4, 7]. The factor responsible for the selective localization of the coordinated phosphonate ligands into metastatic lesions is their affinity for calcium in actively growing bones. The binding energy of interaction between TDTMP and calcite surfaces is -345.4 kcal/mol compared to -294.7 kcal/mol in the case of EDTMP [17] and therefore expected to have higher selectivity. Additionally, TDTMP has higher inhibition potency as it has longer alkyl chain backbone connecting its two N atoms [17].

Experimental

Materials

Ytterbium-176 oxide ($^{176}Yb_2O_3$, spectroscopic grade, 99.7 % pure) was purchased from Aldrich chemical company. Tetra methylene diamine tetra (methylenephosphonic acid) [TDTMP, Mw = 464.177, 99.9% pure) was obtained from REDA Chemicals. Other reagents and chemicals were of high purity grade and were purchased from Sigma-Aldrich or Merck. For electrophoresis and paper chromatography studies, Whatman 3MM chromatography paper (UK) was used. The processed ^{177}Lu radionuclidic purity was ascertained using a High Purity Germanium (HPGe) Detector coupled to a 4 K Multi Channel Analyzer system. Radioactivity measurements were performed using a well type NaI (Tl) scintillation counter. Female Wistar rats were used for animal studies.

Production of ^{177}Lu

The nitrate target was prepared by dissolving 100 mg of $^{176}Yb_2O_3$ in nitric acid with heating, and then evaporating the acid to dryness in T21 quartz vials under vacuum. Then,^{177}Lu was produced by thermal neutron activation at a thermal flux of $1x10^{14}$ n cm^{-2} s^{-1} for 5 days in the 22 MW water cooled Egyptian Research reactor (ETRR-2) and the cooling time was 2 days. Thereafter, the irradiated powder was dissolved in 5 mL of 0.1 M HCl by gentle warming. Separation of ^{177}Lu was achieved using DOWEX 50WX8 cation exchange resin percholated with 50 mL of the proper eluent (0.1 M HCl and 0.25 M α-HIBA, pH adjusted to 3.2 by ammonium hydroxide [18, 19]. The flow rate was 5 drops per min. The resultant solution was evaporated to near dryness and reconstituted in 5 mL of double distilled water and counted on dose calibrator CRC-12R.

Preparation of ^{177}Lu-TDTMP complex and yield optimization

The ^{177}Lu-TDTMP complex was prepared by dissolving the ligand in double distilled water followed by the addition of $^{177}LuCl_3$ (243 µCi) solution. The pH of the resulting mixture was adjusted to 8 using the appropriate buffer and a saline solution was added to complete the final volume to 1 mL. Then, the reaction mixture was incubated at room temperature.

Aiming to achieve maximum complexation yield, several experiments were performed by varying the different reaction parameters such as ligand concentration (1-10 mg), ligand to radiometal ratio (1:1 – 1:50), pH (3-12) and reaction time (5-30 min).

Quality control

The radiolabelling yield of ^{177}Lu-TDTMP was determined by employing paper chromatography and paper electrophoresis techniques as follows:

Paper chromatography

Aliquot of the reaction mixture (5 µL) was spotted at 1.5 cm from the end of Whatman 3mm chromatography paper strips (12x2 cm) and ammonia: ethanol: water (1:10:20) were used as developing solvent. Thereafter, the strips were dried, cut into segments of 1 cm and the activity was measured.

Paper electrophoresis

The labelled formulation (5 µL) was spotted on pre-equilibrated Whatman 3mm chromatography paper strips (35x2 cm) at 1.5 cm from the cathode. Paper electrophoresis was conducted for 1 h under a voltage gradient of 10 v/cm using phosphate buffer (0.025 M, pH 7.5). Following development, the strips were dried, cut into segments (1 cm) and the activity was measured.

Stability study

The *in vitro* stability of ^{177}Lu-TDTMP was studied by storing the complex at room temperature (25±1℃) and human serum at 37 ℃ for a period of 14 days (> 2 half-lives of ^{177}Lu) after preparation. For the in-serum stability test, the labelled complex (0.5 mL) was incubated with freshly prepared sterile filtered human serum (5 mL) at 37℃ under positive nitrogen pressure. At the appropriate time, samples (100 µL) were withdrawn, treated with ethanol (100 µL) and centrifuged (3000 rpm, 10 min) to precipitate serum proteins. Chromatography were performed for the supernatant. The radiochemical purity was assessed by employing the previously mentioned quality control techniques.

Structure prediction and NMR analysis

ChemBio3D ultra 2014 software was used to predict the structure and generate the optimized geometries of the ^{177}Lu-TDTMP complex by molecular mechanics' calculations using our previously reported method [20, 21]; (a molecular geometry related physiochemical property) was computed and compared with the experimental value to confirm the proposed structure of the complex. Then, ^{1}H NMR analysis was performed using Bruker High Performance Digital FT-NMR Spectrometer Avance III 400 MHz and the software ACD/^{1}D NMR Processor V_{12} was used to process the NMR data, assign correlation and further confirm the proposed structure [22].

Hydroxyapatite binding assay

The assay was performed using the previously reported method [23] with slight modification. Briefly, the saline solution (2 mL, pH 7.4) was added to vials containing 1, 2, 5, 10, 20, and 50 mg of solid hydroxyapatite and the mixtures were shaken for 1 h at room temperature. Thereafter, ^{177}Lu-TDTMP (1 mL, 243 µCi) was added and the mixtures were shaken for 24 h followed by centrifugation (3000 rpm, 2 min). Samples (100 µL) were withdrawn from each vial supernatant and the radioactivity was measured using a well-type gamma counter. Blanks were prepared under the same experimental conditions, except the presence of hydroxyapatite,. The complex percentage binding to hydroxyapatite (CBHA) was calculated using the following formula: $CBHA = 1 - A / B \times 100$, where A is the mean radioactivity value of the supernatant sample under study and B is the mean value of blanks.

Partition coefficient

The ^{177}Lu-TDTMP lipophilicity was determined using our previously reported procedure [20] by measuring the activity that partitioned between 1-octanol and sodium phosphate buffer (0.1M,pH 7.4) .At room temperature,1-octanol (2ml), phosphste buffer (1.8 mL) and the labelled complex (0.2 mL) were vortexed in a centrifuge tube for 3 min followed by centrifugation at 2000 rpm for 5 min. Samples (0.1 mL), in triplicate, were withdrawn from both organic and inorganic layers and activity was determined by using a well-type gamma counter. The partition coefficient was calculated using the following equation: Log P = (cpm in octanol − cpm in background) / (cpm in phosphate buffer − cpm in background).

Molecular docking to target enzyme

The iGemDock $V_{2.1}$ software was used to perform molecular docking of the ^{177}Lu-TDTMP into target farnesyl pyrophosphate synthase enzyme and to assess the tracer binding energy and affinity to the binding site at the enzyme. Then, post docking analysis was performed to find the optimum docking pose and its energy values. Structural format of the active conformation the farnesyl pyrophosphate synthase enzyme (PDB ID: 1RQI) was obtained from the protein data bank of the Research Collaboratory for Structural Bioinformatics (RCSB**)** [24]. The complex was subjected to accurate docking and docking parameters were as follows; population size of 800 with 80 generations and 1 solution.

Animal studies, cancer model and biodistribution

Animal experiments were conducted in accordance with the Egyptian Atomic Energy Authority (EAEA) animal welfare institutional guidelines and with the permission of the local animal research committee at the Labelled Compounds Department. Female Wistar rats weighing 200 ± 15 g (mean ± SD, N = 27) were used. Rats were allowed to acclimate for one week before conducting any experiments, maintained in controlled lightening environment, four to a cage and given food and water ad libitum.

Cancer model

A rat model for bone cancer was developed using the previously reported technique [25]. Briefly, under complete anaesthesia, a rostro-caudal incision was made and the tibia was carefully exposed. The bone is pierced 5 mm below the knee joint distal to the epiphyseal growth plate using a 23-gauge needle, then, using Hamilton screw-on metal blunt needle (code 80477) attached to a 10 µL Hamilton syringe, intra-tibial injection of MRMT-1 cancer cells (3 µL, ~3 x 10^3 cells) was performed while simultaneously lifting the needle out of the bone to enable the cells to fill the space. Ultimate care was taken so that no cells leakage occurs outside the bone. Thereafter, metal skin clips were used to close the wound dusted by antibiotic powder. Animals were maintained on heated pad until regaining consciousness before being returned to their cages. Control animals were subjected to the same operation and 3 µL sterile saline solution was injected into the bone.

Biodistribution

One week after tumour induction, rats were injected with 0.2 ml of the labelled complex (243 µCi) through the tail vein. After 3, 24 h and 48 h post injection, animals were anaesthetized and sacrificed by cardiac puncture. Three rats were used for each time point. Tissues and organs were excised, rinsed with normal saline, weighed and counted for activity using γ- counter SR-7. Then, the distribution of activity in different organs was calculated as the percentage of injected activity **(%** ID/g).

Results and Discussion

Production and identification of ^{177}Lu

^{177}Lu (147 mCi) was produced by irradiating ^{176}Yb target (100 mg) at high thermal flux of $1x10^{14}$ n cm^{-2} s^{-1}. After a cooling period of 2 days and following chemical processing, the γ-ray spectrum of irradiated ^{176}Yb target did not show any significant peak corresponding to the photopeaks of ^{177}Yb and exhibited only all the characteristic γ photopeaks of ^{177}Lu (72, 113, 208, 250 and 321 keV), Fig. (1). The radionuclidic purity of the ^{177}Lu was ~100% as confirmed by the γ-ray spectrum owning to chemical processing and the short half-life of trace ^{177}Yb.

Labeling and yield optimization

Radiolabeling conditions were optimized to obtain maximum complexation yield by varying reaction parameters. The optimum labelling yield was obtained by dissolving the ligand [8.4 µg, 18.2 nanoM], Figure (2), in 0.4mL water followed by the addition of $^{177}LuCl_3$ solution [243 µCi of ^{177}Lu activity, 1.59 µg (0.9 nanoM) of Lu]. After adjusting the pH to 8 using $NaHCO_3$ buffer (0.5M, pH 8), the saline solution was added to complete the final volume to 1 mL. The reaction mixture was subsequently incubated at room temperature for 30 min.

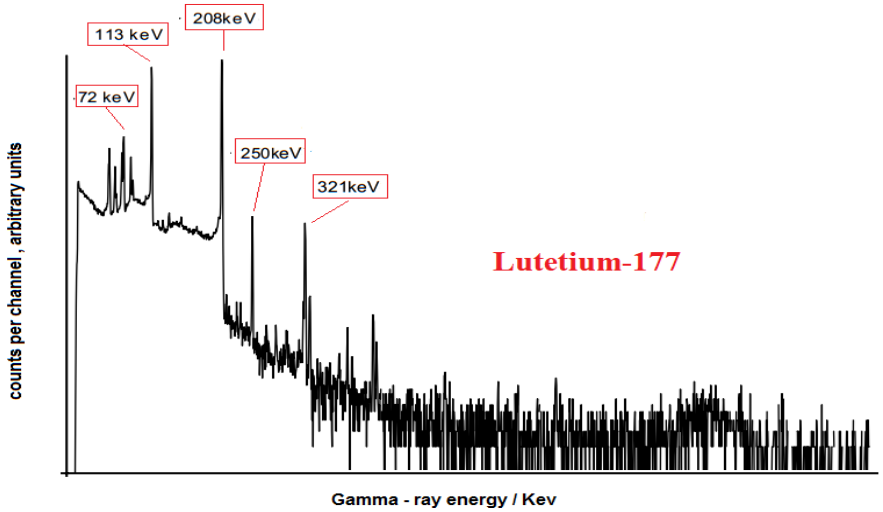

Figure (1): Gamma-ray spectrum of separated ^{177}Lu

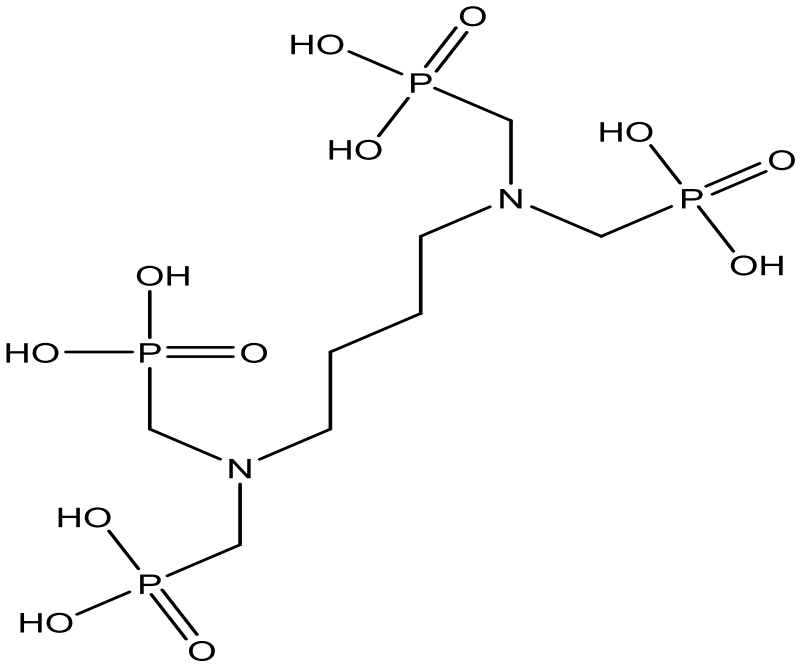

Figure (2): Schematic representation of TDTMP structure

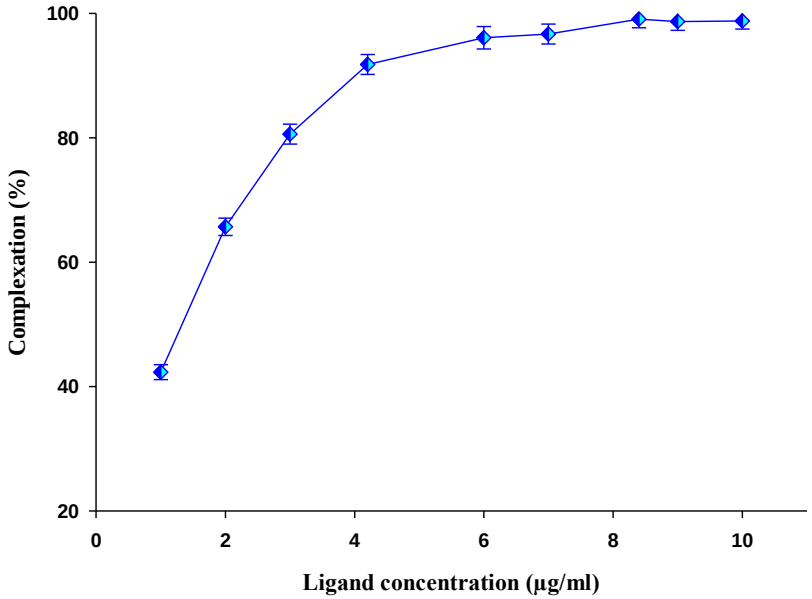

Figure (3): Effect of ligand concentration on complexation yield. Reaction conditions: X µg TDTMP, ~243µCi of ^{177}Lu activity, pH 8, the reaction mixture was kept at room temperature for 30 min

The effect of ligand concentration on complexation yield was studied and the results are shown in Fig. (3). The maximum complexation yield (99.1 %) was achieved using 8.4 µg TDTMP and ~ 243 µCi of ^{177}Lu activity corresponding to a metal to ligand ratio of 1:2. At lower ligand amount the labelling yield was poor. The effect of ligand to metal ratio was also studied and the complexation yield at various metal/ligand ratios is shown in Table (1). No significant variation in radiochemical yield was detected in the range of molar ratios (1:5 to 1:50). However, even if the radiochemical yield of the compound is not affected by the molar ratio in this range (chelating agent/radioisotope), it is sometimes observed that at low molar ratios the *in vivo* behavior may change and liver uptake may increase to levels higher than 1% [26]. A molar ratio of 1/5 (Lu/ TDTMP moles) was chosen for *in vivo* studies. It is also noteworthy that a reasonably good complexation yield of (95.3 ± 0.4) % was obtained using equimolar ratio of Lu and TDTMP. This implies that even low specific activity ^{177}Lu could be used for the preparation of large number of patient doses using correspondingly small amount of ligand relative to the mass of lutetium; an important merit.

Table (1): Complexation yields of ^{177}Lu- TDTMP complex at various Lu-177: ligand ratios

Lu-177 : Ligand	Complexation yield (%)
1:1	95.3 ± 1.1
1:2	97.2 ± 0.3
1:5	98.9 ± 0.8
1:10	99.1 ± 0.5
1:50	99.1 ± 0.4

Mean ± Standard deviation (n = 3

The relation between the pH and the labelling yield was studied in the range from 3 to 12 and maximum yield was obtained at pH 8. As shown in Fig. (4), the yield was low at acidic pH probably due to the dissociation of the Lu-177 from the ligand. Increasing the pH above 9 resulted also, in a decreased yield due to the formation of insoluble Lutetium hydroxide [7]. Figure (5) shows the effect of reaction time on the ^{177}Lu-TDTMP yield. Increasing the reaction time from 5 to 30 min significantly increase in the labeling yield from 46 to ~99 %. Further increasing the reaction time did not affect the complexation yield.

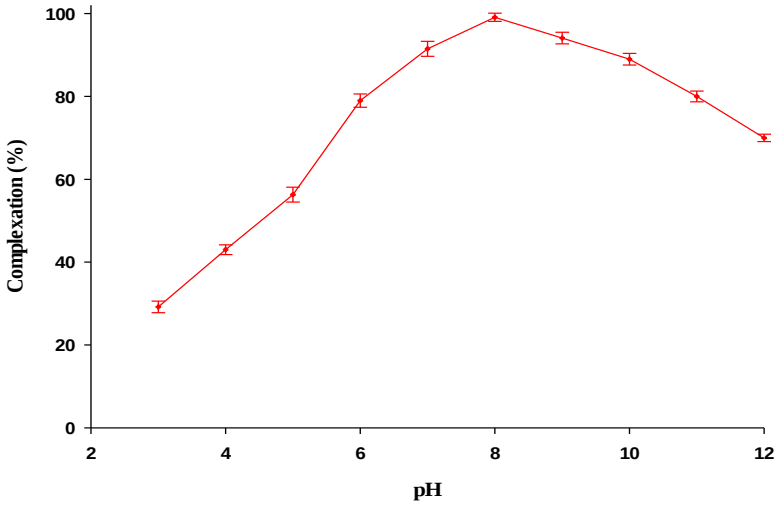

Figure (4): Effect of pH variation on complexation yield. Reaction conditions: 8.4 µg TDTMP, ~243 µCi of ^{177}Lu activity, pH= X, the reaction mixture was kept at room temperature for 30 min

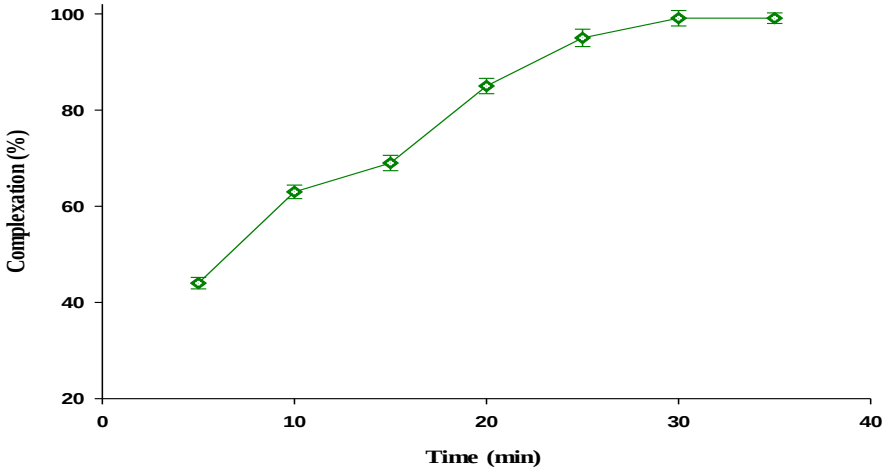

Figure (5): Effect of reaction time on complexation yield. Reaction conditions: 8.4 µg TDTMP, ~243 µCi of ^{177}Lu activity, pH= 8, the reaction mixture was kept at room temperature for different time intervals

Characterization of ^{177}Lu-TDTMP

A combination of paper chromatography and paper electrophoresis techniques were used to characterize the ^{177}Lu-TDTMP complex and ascertain its yield and radiochemical purity. In paper chromatography using ammonia: ethanol: water (1: 10: 20) as a solvent, the complex moved towards the solvent front (R_f = 0.9). On the other hand, under identical conditions the uncomplexed $^{177}LuCl_3$ remained at the point of application (R_f = 0). In paper electrophoresis using phosphate buffer (0.25 M, pH 7.5), it was observed that the complex moved towards the anode indicating that it is negatively charged while the $^{177}LuCl_3$ did not show any appreciable movement from the point of spotting.

Structure prediction and NMR analysis

Lutetium is the last member of the lanthanide series and has electronic configuration [Xe] $4f^{14}$ $5d^1$ $6s^2$. In chemical reaction, it generates a +3 metal cation by losing the 6S and the 5d electrons. Its f orbital is completely filled with electrons that are tightly bound and incapable of bond formation. The ionic radius of Lu^{3+} is small (86.1 pm), thus

the number of ligands that can bind Lu^{3+} are limited and the coordination number is dictated by the repulsions between the various ligands.

The complex cold analogue was prepared and subjected to ^{1}H NMR analysis and the NMR data was assessed and structurally correlated using ACD/^{1}D NMR Processor V_{12}. Results are shown in Fig. (6 a). A computer software, ChemBio3D ultra 2014, was initially used to predict the three dimensional energy optimized structure of ^{177}Lu-TDTMP using molecular mechanics, as shown in Fig. (6 b) The complex is expected to have a tetrahedral geometry with metal: ligand ratio of 1:2 using intermolecular complexation by the bidentate ligand.

Stability study

It was observed that the ^{177}Lu-TDTMP complex was stable at room temperature. Even after 14 days under above-mentioned conditions, the complex was found to retain its radiochemical purity to an extent greater than 98%. The stability test was also developed for the complex in the presence of human serum at 37°C. The chromatogram for the labelled complex did not show any new radiochemical species other than those at expected R_f. At all-time intervals all data were ≥ 95%.

Hydroxyapatite binding assay

The osteoblasts synthesize the bone proteins, mostly collagen and mineralize the bone with hydroxyapatite $[Ca_{10}(PO_4)_5(OH)_2]$, a hard inorganic salt constituting ~ 50-60 % of the human and attributing the skeleton its solid strength. The affinity of the labelled complex to hydroxyapatite is a crucial property responsible for its selective localization into bone metastatic lesions. The result of the binding assay clearly demonstrated high capacity binding of the hydroxyapatite for the ^{177}Lu-TDTMP complex. More than 92 % and 97 % binding were observed at 2 and 5 mg of hydroxyapatite, respectively.

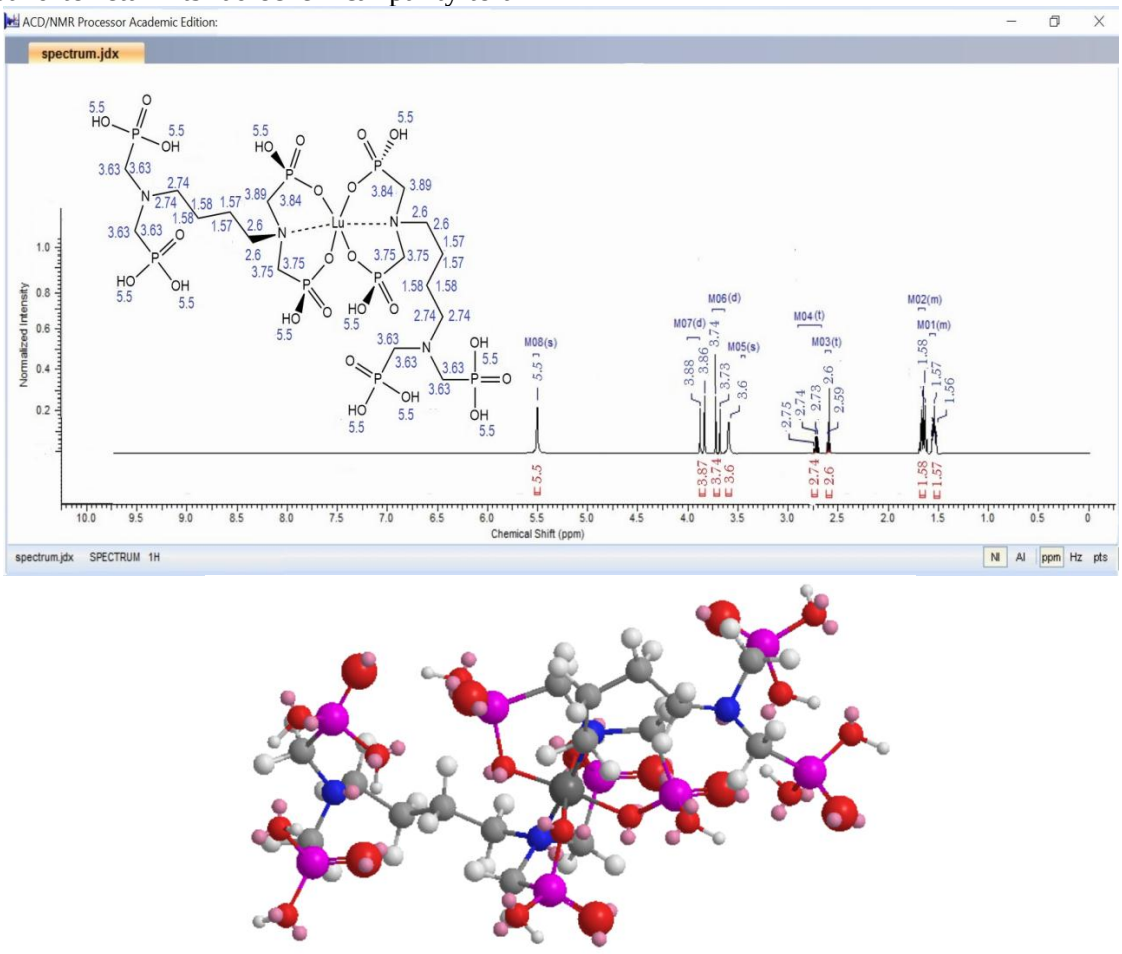

Figure (6): (a) Correlation assignment of ^{177}Lu-TDTMP nuclear magnetic resonance data. (b) Energy optimized proposed structure of the ^{177}Lu-TDTMP complex

Partition coefficient

In preclinical studies, lipophilicity is an important criterion used for decision making on drug likeness of chemical candidates. Whereas the partition coefficient strongly affects the drugs distribution within the body after absorption and as a consequence how rapidly they are metabolized and excreted. Aiming to assess the water/ lipid solubility of the prepared ^{177}Lu-TDTMP complex, the partition coefficient was calculated and found to be -1.5, which indicated the water solubility of the radiocomplex.

Molecular docking to target enzyme

Farnesyl pyrophosphate synthetase (FPPS) synthesizes farnesyl pyrophosphate through successive condensations of isopentyl pyrophosphate with dimethylallyl pyrophosphate and geranyl pyrophosphate. Through conformational changes, the enzyme organizes conserved active site residues to exploit metal-induced ionization and substrate positioning for bone catalysis. Nitrogen-containing bisphosphonate drugs such TDTMP mimic a carbocation intermediate and are potent inhibitors of the enzyme. The affinity of the labelled phosphonate ligand for calcium in activity growing bones is considered to be responsible for their selective localization into metastatic lesions [27, 28].

To evaluate the binding of the ^{177}Lu-TDTMP to its target, FPPS enzyme, docking was performed using iGemdock software. Based on the expected Van Der Waal's, hydrogen-bonding and electrostatic interactions, the accurate flexible docking results, illustrated in Fig. (7), indicated that the labelled compound has an optimal fit with a binding energy of −124.7 Kcal/mole. The interaction profile of the complex and its best docking pose with the FPPS enzyme are illustrated in Fig. (7) which also shows the coordinates of the labelled compound atoms interacting with their respective amino acids of the target enzyme.

Cancer model

A rat model for bone cancer was developed using the reported technique [29]. Briefly, under complete anaesthesia, a rostro-caudal incision was made and the tibia was carefully exposed. The bone is pierced 5 mm below the knee joint distal to the epiphyseal growth plate using a 23-gauge needle. Then using Hamilton screw-on metal blunt needle (code 80477) attached to a 10 µL Hamilton syringe, intra-tibial injection of MRMT-1 cancer cells (3 µL, ~3 x 10^3 cells) was performed while simultaneously lifting the needle out the bone to enable the cells to fill the space. Ultimate care was taken so that no cells leakage occurs outside the bone. Thereafter, metal skin clips were used to close the wound dusted by antibiotic powder. Animals were maintained on heated pad until regaining consciousness before being returned to their cages. Control animals were subjected to the same operation and 3 µL sterile saline solution was injected into the bone.

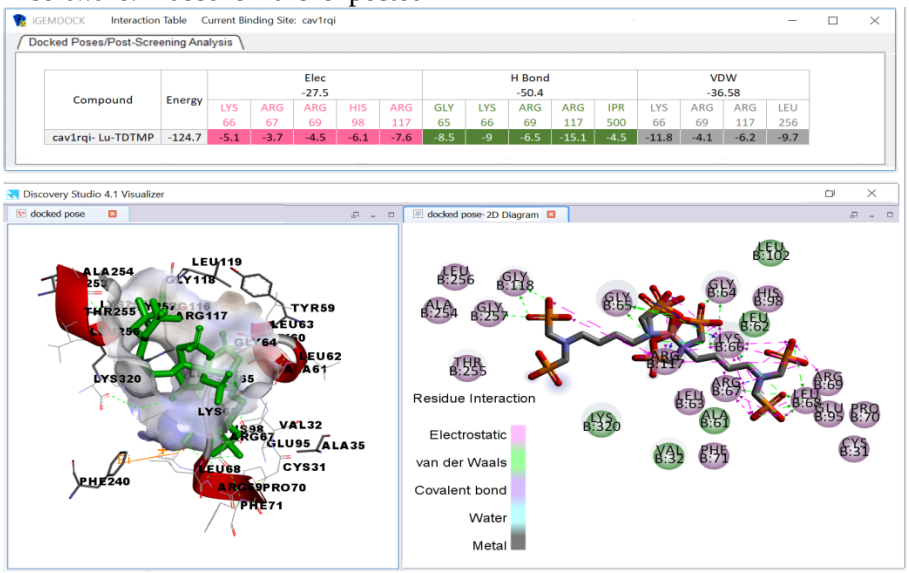

Figure (7): Docking pose and interaction profile analysis of the ^{177}Lu-TDTMP with the Farnesyl pyrophosphate synthetase target

Biodistribution study

Biological evaluation of ^{177}Lu-TDTMP was determined in normal and tumor induced female Wistar rats for 3, 24 and 48 h post injection. In addition, the biodistribution of the labelled complex was compared with the biodistribution of $^{177}LuCL_3$ in normal rat to assess the effect of complexation on the Lu-177. Results of the current study are presented in Table (2). For the $^{177}LuCl_3$, the liver uptake was significant; ~ 2.9 % accumulation at 48 hours post injection. The spleen also showed considerable uptake (~ 3.15 % and ~1.343 % at 24 and 48 h, respectively) possibly related to reticuloendothelial system. The biodistribution of the Lu^{3+} cation is in line with the previously reported results [30]. For the ^{177}Lu-TDTMP, results clearly indicated that it has high affinity for bone mineral. Femur and tibia uptakes of the labelled complex were ~ 6.4 % and ~7.1 % at 3 hours post injection compared to ~ 4 % and ~ 4.3 % in case of $^{177}LuCl_3$. Thereafter, the uptakes increased continuously to a maximum of ~ 7.9 % and ~ 8.3 % at 48 hours after injection. Because of water solubility of radiocomplex, it was observed in the kidneys in the first hours post injection reflecting the route of excretion. However, the kidneys uptake washed out rapidly from ~ 3.4 % ID/g at 3 hours to ~ 0.27 % ID in 24 hours post injection. Apart from this, no significant uptake was demonstrated in any other organ or tissue. In the tumor-induced model, the labelled complex showed a similar organs distribution with the exception of the tumorised tibia uptake which was ~14.5 %, ~15.7 % and ~16.4 % at 3, 24 and 48 h post injection. No leaching of the bone activity was observed as there was no increment in the uptake in any organ. It was noted that in both the normal and tumour-bearing model, almost all the activity was cleared from blood within 3h post injection indicating that a good scintigraphic image would be obtained as a target holding a high activity for comparison with the blood pool (general background). The bone –muscle uptake ratios of the labelled compound was calculated and found to be more than 21 from 3 to 48 h. This is an important factor for therapeutic radiopharmaceutical to reduce unwanted irradiation doses to the patients. The bone-liver ratio, an equally significant target to non-target criterion for the efficacy of bone agents, was also calculated and results are presented in Table (3). The values of the complex uptake in blood, liver and tibia were compared to those of ^{177}Lu-EDTMP, ^{177}Lu-TTHMP and ^{177}Lu-DTPMP in normal Wistar rat Table (4) [15]. As evident from the results, ^{177}Lu-TDTMP has higher skeletal uptake and lower liver accumulation [31].

Conclusion

In the present study, the possibility of developing a theranostic agent for bone metastases was explored by labelling a phosphonate bone-seeking agent (TDTMP) with the radionuclide ^{177}Lu. ^{177}Lu-TDTMP could be useful for both diagnosis and therapy of multiple bone metastases. Therapeutic effect would be the synergy of an enhanced accumulation of osteotropic agents and the energy deposit by the emitted β-particles on the metastatic lesion. Additionally, ^{177}Lu emits γ photons that are quite suited for diagnosis and imaging the *in vivo* localization.

^{177}Lu- TDTMP complex was prepared in a high yield and excellent radiochemical purity using ^{177}Lu produced by thermal neutron irradiation of ^{176}Yb in the Egyptian Research reactor (ETRR-2). The complex, prepared using optimized conditions, exhibited excellent *in-vitro* stability and optimal fit with the target Farnesyl pyrophosphate synthetase enzyme. Results of the *in vitro* binding study with the hydroxyapatite and the *in vivo*, bio-localization characteristics of the complex (selective lesion affinity, high bone uptake, rapid blood clearance and almost no uptake in any of the major organs/tissue) strongly suggested the usefulness of the tracer. Based on the preliminary preclinical evaluation, ^{177}Lu-TDTMP has promising characteristics and could be a more effective candidate for targeting bone metastases as compared to others phosphonates. This warrants further biological studies in higher animals prior to starting prophase I clinical studies in human.

Table (2): Biodistribution of $^{177}LuCl_3$ in normal rats and of ^{177}Lu-TDTMP in normal and tumor bearing rat model (%ID/g)

Organs/tissues	Distribution (in %) at different intervals (in hours)								
	$LuCl_3$ in normal rat			^{177}Lu-TDTMP in normal rat			^{177}Lu-TDTMP in tumor bearing rat		
	3	24	48	3	24	48	3	24	48
Blood	0.4 ± 0.0	0.1 ± 0.0	0.00 ± 0.0	0.1 ± 0.0	0.1 ± 0.0	0.00 ± 0.0	0.3 ± 0.0	0.1 ± 0.0	0.00 ± 0.0
Liver	5.67 ± 0.4	4.57 ± 0.3	2.90 ± 0.1	0.15 ± 0.0	0.08 ± 0.0	0.06 ± 0.0	0.15 ± 0.0	0.07 ± 0.0	0.06 ± 0.0
Intestine	1.44 ± 0.2	0.14 ± 0.0	0.1 ± 0.0	0.42 ± 0.2	0.14 ± 0.0	0.1 ± 0.0	0.42 ± 0.1	0.14 ± 0.0	0.09 ± 0.0
Kidneys	4.52 ± 0.5	2.82 ± 0.3	2.65 ± 0.2	3.36 ± 0.3	0.27 ± 0.1	0.28 ± 0.0	3.31 ± 0.3	0.27 ± 0.0	0.28 ± 0.0
Stomach	0.06 ± 0.0	0.00 ± 0.0	0.00 ± 0.0	0.06 ± 0.0	0.00 ± 0.0	0.00 ± 0.0	0.06 ± 0.0	0.00 ± 0.0	0.00 ± 0.0
Heart	0.2 ± 0.0	0.1 ± 0.0	0.00 ± 0.0	0.1 ± 0.0	0.00 ± 0.0	0.00 ± 0.0	0.1 ± 0.0	0.00 ± 0.0	0.00 ± 0.0
Lungs	0.03 ± 0.0	0.01 ± 0.0	0.00 ± 0.0	0.01 ± 0.0	0.00 ± 0.0	0.00 ± 0.0	0.01 ± 0.0	0.00 ± 0.0	0.00 ± 0.0
Muscles	0.2 ± 0.0	0.1 ± 0.0	0.00 ± 0.0	0.1 ± 0.0	0.00 ± 0.0	0.00 ± 0.0	0.1 ± 0.0	0.00 ± 0.0	0.00 ± 0.0
Spleen	2.47 ± 0.3	3.15 ± 0.4	1.34 ± 0.1	0.00 ± 0.0	0.00 ± 0.0	0.00 ± 0.0	0.00 ± 0.0	0.00 ± 0.0	0.00 ± 0.0
Urine	58.78 ± 1.8	61.76 ± 1.9	67.52 ± 0.8	49.67 ± 1.5	57.83 ± 1.6	58.54 ±0.9	49.67 ± 1.4	57.83 ± 1.8	58.54 ± 0.9
Femur	3.96 ± 0.3	4.12 ± 0.4	4.73 ± 0.2	6.44 ± 0.2	6.53 ± 0.8	7.78 ± 0.3	6.44 ± 0.2	6.53 ± 0.9	7.84 ± 0.3
Tibia	4.35 ± 0.6	4.94 ± 0.5	5.43 ± 0.4	7.13 ± 0.6	7.87 ± 0.6	8.31 ± 0.1	14.53 ± 0.6	15.65 ± 0.4	16.35 ± 0.1

Mean ± Standard deviation (n = 3)

Table (3): Target (Tibia): Non-target ratios for ^{177}Lu-TDTMP in normal and tumor-bearing rat model at various time intervals

Time / Ratio	Post injection time (hours)								
	$LuCl_3$ in normal rat			^{177}Lu-TDTMP in normal rat			^{177}Lu-TDTMP in tumor bearing rat		
	3	24	48	3	24	48	3	24	48
Target/Blood	10.86	49.4[a]	543.1[a]	17.83	74.65[a]	831[a]	48.44	156.53[a]	1635.1[a]
Target/Muscle	21.73	49.42[a]	543.1[a]	71.33	746.5[a]	831	145.33	1565.3[a]	1635.1[a]
Target/Liver	0.76	1.08[a]	1.87[a]	49.19	99.53[a]	136.22	98.86	214.42[a]	277.13[a]
Tibia/Femur	1.09	1.2	1.15	1.1	1.15	1.09	2.26	2.4	2.09

[a] Significantly different from previous time point value

Table (4): Comparison of blood, liver and Tibia uptake pattern of ^{177}Lu-TDTMP, ^{177}Lu-EDTMP, ^{177}Lu-TTHMP and ^{177}Lu-DTPMP in Wistar rats(%ID/g)

Organs/tissues	Distribution (in %) at different intervals (in hours) in Wistar Rat											
	^{177}Lu-TDTMP			^{177}Lu-EDTMP			^{177}Lu-TTHMP			^{177}Lu-DTPMP		
	3	24	48	3	24	48	3	24	48	3	24	48
Blood	0.1 ± 0.0	0.1 ± 0.0	0.00 ± 0.0	0.0 ± 0.0	0.0 ± 0.0	0.00 ± 0.0	0.1 ± 0.0	0.0 ± 0.0	0.00 ± 0.0	0.4 ± 0.0	0.0 ± 0.0	0.0 ± 0.0
Liver	0.15 ± 0.0	0.08 ± 0.0	0.06 ± 0.0	0.16 ± 0.0	0.12 ± 0.0	0.16 ± 0.0	0.15 ± 0.1	0.13 ± 0.0	0.13 ± 0.0	0.32 ± 0.2	0.21 ± 0.1	0.25 ± 0.1
Tibia	7.13 ± 0.6	7.87 ± 0.6	8.31 ± 0.1	6.51 ± 0.2	7.71 ± 0.7	6.72 ± 1.1	6.58 ± 1.14	7.28 ± 0.3	6.93 ± 2.7	6.16 ± 0.74	6.25 ± 0.7	7.26 ± 0.8

Mean ± Standard deviation (n = 3)

References

1-R. Bergmann, M. Meckel, V. Kubíček, J. Pietzsch, J. Steinbach, P. Hermann, F. Rösch F, *EJNMMI Research*. 2016, 6(5), 1–12.
2-N. Salek, M. Mehrabi, S. Arani, A. Samani, M. Erfani, S. Vosoghi, M. Maragheh, M. Shamsaei, *J Label Compd Radiopharm*. 2017, 60(1), 20–29.
3-S. Zolghadri, H. Yousefnia, A. Jalilian, M. Ghannadi-Maragheh, *J Nucl Med Biol*. 2015, 3(1), 35–42.
4-H. Yousefnia, S. Zolghadri, S. Shanehsazzadeh, *Appl Rad and Isotopes*. 2015, 104 ,128–135.
5-O. Nielsen, A. Munro, I. Tannock, *J Clin Oncol*. 1991, 9, 509–524.
6-M. Ignatiadis, C. Sotiriou, *Nat Rev Clin Oncol*. 2013, 10, 494–506.
7-T. Das, S. Chakraborty, P. Unni, S. Banerjee, G. Samuel, H. Sarma, M. Venkatesh, M. Pillai, *Appl Rad and Isotopes*. 2002, 57, 177–184.
8-M. Graham, H. Scher, G. Liu, S. Yeh, T. Curley, F. Daghighian, S. Goldsmith, S. Larson, *Clin Can Res*. 1999, 5, 1307–1318.
9-J. Jones, S. Lutz, E. Chow, P. Johnstone, *Can J Clin*. 2014, 64, 295–310.
10-S. Lutz, T. Balboni, J. Jones, S. Lo, J. Petit, S. Rich, R. Wong, C. Hahn, *Pract Rad Oncol*. 2017, 7, 4–12.
11-E. Koumarianou, R. Mikołajczak, D. Pawlak, X. Zikos, P. Bouziotis, P. Garnuszek, U. Karczmarczyk, M. Maurin, S. Archimandritis, *Nucl Med and Biol*. 2009, 36: 591–603.
12-A. Rabie, R. Enayati, H. Yousefnia, A. Jalilian, M. Shamsaei, S. Zolghadri, A. Bahrami-Samani, M. Hosntalab, *Ann Nucl Med*. 2015, 29, 870–876.
13-H. Mohsin, J. Fitzsimmons, T. Shelton, T. Hoffman, C. Cutler, M. Lewis, P. Athey, G. Gulyas, G. Kiefer, R. Frank, J. Simon, S. Lever, S. Jurisson, *Nucl Med and Biol*. 2007, 34, 493–502.
14-T. Das, S. Chakraborty, H. Sarma, S. Banerjee, *Radiochim Acta*, 2008, 96, 55–61.
15-S. Chakraborty, T. Das, P. Unni, H. Sarma, G. Samuel, S. Banerjee, M. Venkatesh, N. Ramamoorthy, M. Pillai, *Nucl Med Com*. 2002, 23, 67–74
16-N. Salek, M. Shamsaei, M. Maragheh, S. Arani, A. Samani, J Nucl Med. 2017, 25(1), 23–33.
17-W. Lei, C. Chen, N. Bai, *Int Conf Mat Sci and Appl*. 2015, Doi: 10.2991/icmsa-15.2015.93.
18-A. Dash A, R. Chakravarty, F. Jr, A. Pillai, *Curr Radiopharm*. 2015, 8, 107–118.
19-A. Dash, M. Pillai, F. Jr, *Nucl Med Mol Imaging*. 2015, 49, 85–107. A. Gisela. R. Sola, M. Argüelles, D. Bottazzini, J. Furnari, I. Parada, A. Rojo, H. Ruiz, *Radiochim Acta*. 2000, 88, 157–161.
20-O.A. El-Kawy, I. Ibrahim, K. Farah, *J Label Compd Radiopharm*. 2015, 58, 336–341.
21-O.A. El-Kawy, J. García-Horsman, R. Tuominen, *Appl Rad and Isotopes*. 2016, 118, 258–265.
22-O.A. El-Kawy, J. García-Horsman, *J Radioanal Nucl Chem*. 2017, 314, 2539–2550.
23-O.A. El-kawy, A. Abdel-Razek, M. Sayed, *J Radioanal Nucl Chem*. 2016, 308, 1081–1088.
24-M. Nevesa, L. Ganoa, N. Pereiraa, M. Costab, M. Chandiac, M. Rosadod, R. Faustod, *Nucl Med and Biol*. 2002, 29, 329–338.
25-D. Hosfield, Y. Zhang, D. Dougan, A. Brooun, L. Tari, R. Swanson, J. Finn, *J Biol Chem*. 2004, 279, 8526–8529.
26-S. Medhurst, K. Walker, M. Bowes, B. Kidd, M. Glatt, M. Muller, M. Hattenberger, J. Vaxelaire, T. O'Reilly, G. Wotherspoon, J. Winter, J. Green, L. Urban, *Pain*. 2002, 96(1), 129–140.
27-A. Gisela. R. Sola, M. Argüelles, D. Bottazzini, J. Furnari, I. Parada, A. Rojo, H. Ruiz, *Radiochim Acta*. 2000, 88, 157–161.
28-M.S, Tamer, A.K., Mohammed M.R, Hassan and E. M Maged, In Silico-Based Repositioning of Phosphinothricin as a Novel Technetium-99m Imaging Probe with Potential Anti-Cancer Activity, Molecules, 2018, 23, 496.
29-F. Johari, S. Shafiei, S. Sheibani, Y. Tavakoli, M. Mazidi, M. Mirfalah, M. Babaei, *IJRR*. 2010, 7(4), 229–234.

30-H. Yousefnia, A. Jalilian, A. Bahrami-Samani, M. Mazidi, M. Maragheh, F. Abbasi-Davani, Iran J Basic Med Sci. 2013, 16(5), 705–709.

31-T. Philipp, H. Jochen, H. Melanie, W. Markus, S. Klaus, K. Carsten, P. David, H. Axel, D. Markus, S. Matthias, and D. Alexander. Discrete evaluation of multi-cycle Lu-177-PSMA-617-therapy effects on bone versus lymph node metastases in patients with metastasized castration‑ resistant prostate cancer (mCRPC) J. Nucl. Med May 1. 2018 ,vol. 59:523